

Dear Dr. Luterbacher,

My coauthors and I thank you for your invitation to revise our manuscript. Here we will comment on, one-by one, the referee comments/suggestions.

Sincerely,  
Nesibe Köse

### **Response to RC1 comments**

Thank you for your time and comments. We would like to thank you for your time and comments.

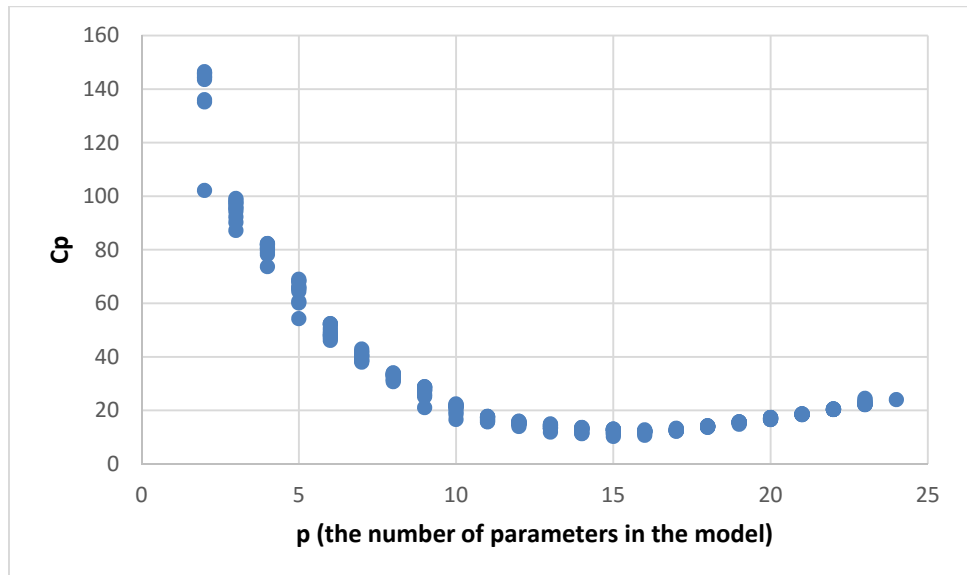
General comments:

We could not use only the chronologies that have significant relationship to temperature, because at the same time they have significant precipitation signal (except ART chronology, Figure 2). On the other hand, we would like to show that it is possible to make a climate reconstruction from a tree-ring network, even if this climate variable is not the most important limiting factor on radial growth. In our case, May to August precipitation was the most important factor, and the second one was March-April TMP for almost all the chronologies. Classical approach in Dendroclimatology, is to use the PC 1 and/or high order PCs reconstruct precipitation. But here, we would like show that PC 1 could be a signal for precipitation but a noise for temperature. On the other hand the other PC's, which explain less variance, could be noise for precipitation and but a signal for temperature.

Specific Comments:

1. Thank you for your attention we corrected it in the manuscript.
2. We cited the investigators produced the chronologies.
3. We replaced the sentence by: "Third, the final reconstruction is based on bootstrap regression (Till and Guiot, 1990), a method designed to calculate appropriate confidence intervals for reconstructed values and explained variance even in cases of short time-series."
4. We will replace by "... but bootstrap has the advantage to produce confidence intervals for such statistics without theoretical probability distribution and finally we accept the RE and CE for which the lower confidence margin at 95% are positive. This is more constraining than just accepting all positive RE and CE."
5. We added information in the text under the titles "Data and Method", "Temperature reconstruction" explaining which method we used stepwise regression. We combined forward selection with backward elimination, checking for entry, then removal, until no more variables can be added or removed. Each procedure requires only that we set significance levels (or critical values) for entry and/or removal. We used  $p \leq 0.05$  as entrance tolerance and  $p \leq 0.1$  as exit tolerance. Actually, for almost all PCs it was  $p \leq 0.01$  in entire regression. The

final model obtained when the regression reaches a local minimum of RMSE. We also calculated Mallows Cp values. See the relation Cp and p (the number of parameters in the model, including the intercept) in (Figure1) .



We did not use a split-sample procedure to verify the model stability. We used bootstrap method. Therefore we run SR for the whole period. Bootstrap is only applied to the selected set of predictors by stepwise regression. Then it is not concerned by the bootstrap. We did not calculate RE, CE at each step of the stepwise regression. But based on the suggestion of both reviewer, for additional verification we also give split-sample procedure results using the same variables that were suggested for the whole period.

6. We added a column to Table 3, to show the chronologies represented by higher magnitudes of the eigenvectors.

7. We tried to say with this sentence that no temperature reconstruction has been made, which mean that it is difficult to do that.

8. We did suggested changes in the figures.

### **Response to RC2 comments:**

Thank you for your time and valuable comments. We would like to thank you for your time and comments.

1. We give detailed information: “.....to produce time series with a strong common signal and without biological persistence. The residual chronologies may be more suitable to understand the effect of climate on tree-growth, even if any persistence due to climate might be removed by pre-whitening. ..... In this research we used residual chronologies obtained from ARSTAN to reconstruct temperature.

2. We added suggested information “Principle Component Analysis (PCA) was done over the entire period in common to the tree-ring chronologies. The significant PCs were selected by

stepwise regression. We combined forward selection with backward elimination setting  $p \leq 0.05$  as entrance tolerance and  $p \leq 0.1$  as exit tolerance. The final model obtained when the regression reaches a local minimum of RMSE. The order of entry of the PCs into the model was  $PC_3, PC_{21}, PC_4, PC_{15}, PC_5, PC_{17}, PC_7, PC_9, PC_{10}$ .”

3. We replaced the sentence by: “Third, the final reconstruction is based on bootstrap regression (Till and Guiot, 1990), a method designed to calculate appropriate confidence intervals for reconstructed values and explained variance even in cases of short time-series.” We calculate RE and CE values for 1901-29 and obtained low values. Therefore we removed discussion this part from the text and figure. For additional verification we present split calibration/verification results, which you mentioned that it may provide a more religious test, for the period 1930-2002 in Table 5.

4. Eq. (1) was removed as you suggested.

The suggested reference was added.

1    **Spring temperature variability over Turkey since 1800 CE reconstructed**  
2    **from a broad network of tree-ring data**

3

4    **Nesibe Köse<sup>(1)\*</sup>, H. Tuncay Güner<sup>(1)</sup>, Grant L. Harley<sup>(2)</sup>, Joel Guiot<sup>(3)</sup>**

5  
6    <sup>(1)</sup>Istanbul University, Faculty of Forestry, Forest Botany Department 34473 Bahçeköy-Istanbul,  
7    Turkey

8    <sup>(2)</sup>University of Southern Mississippi, Department of Geography and Geology, 118 College  
9    Drive Box 5051, Hattiesburg, Mississippi, 39406, USA

10    <sup>(3)</sup>Aix-Marseille Université, CNRS, IRD, CEREGE UM34, ECCOREV, 13545 Aix-en-  
11    Provence, France

12

13

14

15

16

17    \*Corresponding author. Fax: +90 212 226 11 13

18    E-mail address: [nesibe@istanbul.edu.tr](mailto:nesibe@istanbul.edu.tr)

19

20 **Abstract**

21 The 20<sup>th</sup> century was marked by significant decreases in spring temperature ranges and increased  
22 nighttime temperatures throughout Turkey. The meteorological observational period in Turkey,  
23 which starts *ca.* 1929 CE, is too short for understanding long-term climatic variability. Hence,  
24 the historical context of this gradual warming trend in spring temperatures is unclear. Here we  
25 use a network of 23 tree-ring chronologies to provide a high-resolution spring (March–April)  
26 temperature reconstruction over Turkey during the period 1800–2002. The reconstruction model  
27 accounted for 67% (Adj.  $R^2 = 0.64$ ,  $p \leq 0.0001$ ) of the instrumental temperature variance over the  
28 full calibration period (1930–2002). During the pre-instrumental period (1800–1929) we captured  
29 more cold events ( $n = 23$ ) than warm ( $n = 13$ ), and extreme cold and warm events were typically  
30 of short duration (1–2 years). Compared to coeval reconstructions of precipitation in the region,  
31 our results are similar with durations of extreme wet and dry events. The reconstruction is  
32 punctuated by a temperature increase during the 20<sup>th</sup> century; yet extreme cold and warm events  
33 during the 19<sup>th</sup> century seem to eclipse conditions during the 20<sup>th</sup> century. During the 19<sup>th</sup>  
34 century, annual temperature ranges are more volatile and characterized by more short-term  
35 fluctuations compared to the 20<sup>th</sup> century. During the period 1900–2002, our reconstruction  
36 shows a gradual warming trend, which includes the period during which diurnal temperature  
37 ranges decreased as a result of increased urbanization in Turkey.

38

39 KEYWORDS: Dendroclimatology, Climate reconstruction, *Pinus nigra*, Principle component  
40 analysis, Spring temperature.

41 **1 Introduction**

42

43 Significant decreases in spring diurnal temperature ranges (DTR) occurred throughout Turkey  
44 from 1929 to 1999 (Turkes & Sumer 2004). This decrease in spring DTRs was characterized by  
45 day-time temperatures that remained relatively constant while a significant increase in night-time  
46 temperatures were recorded over western Turkey and were concentrated around urbanized and  
47 rapidly-urbanizing cities. The historical context of this gradual warming trend in spring  
48 temperatures is unclear as the high-quality meteorological records in Turkey, which start in  
49 1929, are relatively short for understanding long-term climatic variability.

50

51 Tree rings have shown to provide useful information about the past climate of Turkey and were  
52 used intensively during the last decade to reconstruct precipitation in the Aegean ([Hughes et al. 2001](#),  
53 Griggs et al. 2007), Black Sea (Akkemik et al. 2005, [2008](#); [Martin-Benitto et al. 2016](#)),  
54 Mediterranean regions (Touchan et al. 2005a), as well as the Sivas (D'Arrigo & Cullen 2001),  
55 southwestern (Touchan et al. 2003, Touchan et al. 2007; [Köse et al. 2013](#)), south-central  
56 (Akkemik & Aras 2005) and western Anatolian (Köse et al. 2011) regions of Turkey. These  
57 studies used tree rings to reconstruct precipitation because available moisture is often found to be  
58 the most important limiting factor that influences radial growth of many tree species in Turkey.  
59 These studies revealed past spring-summer precipitation, and described past dry and wet events  
60 and their duration. Recently, Heinrich et al. (2013) provided a winter-to-spring temperature  
61 proxy for Turkey from carbon isotopes within the growth rings of *Juniperus excelsa* since AD  
62 1125. Low-frequency temperature trends corresponding to the Medieval Climatic Anomaly and  
63 Little Ice Age were identified in the record, but the proxy failed to identify the recent warming

64 trend during the 20<sup>th</sup> century. In this study, we present a tree-ring based spring temperature  
65 reconstruction from Turkey and compare our results to previous reconstructions of temperature  
66 and precipitation to provide a more comprehensive understanding of climate conditions during  
67 the 19<sup>th</sup> and 20<sup>th</sup> centuries.

68

69 **2 Data and Methods**

70 **2.1 Climate of the Study Area**

71

72 The study area, which spans 36–42° N and 26–38° E, was based on the distribution of available  
73 tree-ring chronologies. This vast area covers much of western Anatolia and includes the western  
74 Black Sea, Marmara, and western Mediterranean regions. Much of this area is characterized by a  
75 Mediterranean climate that is primarily controlled by polar and tropical air masses (Türkeş 1996,  
76 Deniz et al. 2011). In winter, polar fronts from the Balkan Peninsula bring cold air that is  
77 centered in the Mediterranean. Conversely, the dry, warm conditions in summer are dominated  
78 by weak frontal systems and maritime effects. Moreover, the Azores high-pressure system in  
79 summer and anticyclonic activity from the Siberian high-pressure system often cause below  
80 normal precipitation and dry sub-humid conditions over the region (Türkeş 1999, Deniz et al.  
81 2011). In this Mediterranean climate, annual mean temperature and precipitation range from 3.6  
82 °C to 20.1 °C and from 295 to 2220 mm, respectively, both of which are strongly controlled by  
83 elevation (Deniz et al. 2011).

84

85

86

87

88 2.2 Development of tree-ring chronologies

89

90 To investigate past temperature conditions, we used a network of 23 tree-ring site chronologies

91 (Fig. 1). Fifteen chronologies were produced by previous investigations ([Mutlu et al. 2011](#),

92 [Akkemik et al. 2008](#), [Köse et al. unpublished data](#), [Köse et al. 2011](#), [Köse et al. 2005](#)) that

93 focused on reconstructing precipitation in the study area. In addition, we sampled eight new

94 study sites and developed tree-ring time series for these areas (Table 1). Increment cores were

95 taken from living *Pinus nigra* Arn. and *Pinus sylvestris* L. trees and cross-sections were taken

96 from *Abies nordmanniana* (Steven) Spach and *Picea orientalis* (L.) Link [treestrunks](#).

97

98 Samples were processed using standard dendrochronological techniques (Stokes & Smiley 1968,

99 Orvis & Grissino-Mayer 2002, Speer 2010). Tree-ring widths were measured, then visually

100 crossdated using the list method (Yamaguchi 1991). We used the computer program COFECHA,

101 which uses segmented time-series correlation techniques, to statistically confirm our visual

102 crossdating (Holmes 1983, Grissino-Mayer 2001). Crossdated tree-ring time series were then

103 standardized by fitting a 67% cubic smoothing spline with a 50% cutoff frequency to remove

104 non-climatic trends related to the age, size, and the effects of stand dynamics using the ARSTAN

105 program (Cook 1985, Cook et al. 1990a). These detrended series were then pre-whitened with

106 low-order autoregressive models-[to produce time series with a strong common signal and](#)

107 [without biological persistence](#)~~to remove persistence not related to climatic variations.~~ [-These](#)

108 [series may be more suitable to understand the effect of climate on tree-growth, even if any](#)

109 [persistence due to climate might be removed by pre-whitening.](#) For each chronology, the

110 individual series were averaged to a single chronology by computing the biweight robust means  
111 to reduce the influences of outliers (Cook et al. 1990b). [In this research we used residual](#)  
112 [chronologies obtained from ARSTAN to reconstruct temperature.](#)

113  
114 The mean sensitivity, which is a metric representing the year-to-year variation in ring width  
115 (Fritts 1976), was calculated for each chronology and compared. The minimum sample depth for  
116 each chronology was determined according to expressed population signal (EPS), which we used  
117 as a guide for assessing the likely loss of reconstruction accuracy. Although arbitrary, we  
118 required the commonly considered- threshold of EPS > 0.85 (Wigley et al. 1984; Briffa & Jones  
119 1990).

120

## 121 2.3 Temperature reconstruction

122

123 We extracted monthly temperature and precipitation records from the climate dataset CRU TS  
124 3.23 gridded at 0.5° intervals (Jones and Harris 2008) from KNMI Climate Explorer  
125 (<http://climexp.knmi.nl>) for 36–42 °N, 26–38 °E. The period AD 1930–2002 was chosen for the  
126 analysis because it maximized the number of station records within the study area.

127

128 First, the climate-growth relationships were investigated with response function analysis (RFA)  
129 (Fritts 1976) for biological year from previous October to current October using the  
130 DENDROCLIM2002 program (Biondi & Waikul 2004). This analysis is done to determine the  
131 months during which the tree-growth is the most responsive to temperature. Second, the climate  
132 reconstruction is performed by regression based on the principal component (PCs) of the 23

133 chronologies within the study area. Principle Component Analysis (PCA) was done over the  
134 entire period in common to the tree-ring chronologies. The significant PCs were selected by  
135 stepwise regression. We combined forward selection with backward elimination setting  $p \leq 0.05$   
136 as entrance tolerance and  $p \leq 0.1$  as exit tolerance. The final model obtained when the regression  
137 reaches a local minimum of RMSE. The order of entry of the PCs into the model was PC<sub>3</sub>, PC<sub>21</sub>,  
138 PC<sub>4</sub>, PC<sub>15</sub>, PC<sub>5</sub>, PC<sub>17</sub>, PC<sub>7</sub>, PC<sub>9</sub>, PC<sub>10</sub>. The regression equation is calibrated on the common  
139 period (1930–2002) between robust temperature time-series and the selected tree-ring series.  
140 ~~Third, the final reconstruction is based on bootstrap regression (Till and Guiot, 1990), the best~~  
141 ~~method to assess the quality of the regression and to calculate appropriate confidence intervals.~~  
142 Third, the final reconstruction is based on bootstrap regression (Till and Guiot, 1990), a method  
143 designed to calculate appropriate confidence intervals for reconstructed values and explained  
144 variance even in cases of short time-series. It consists in randomly resampling the calibration  
145 datasets to produce 1000 calibration equations based on a number of slightly different datasets.  
146 The quality of the reconstruction is assessed by a number of standard statistics. The overall  
147 quality of fit of reconstruction is evaluated based on the determination coefficient ( $R^2$ ), which  
148 expresses the percentage of variance explained by the model and the root mean squared error  
149 (RMSE), which expresses the calibration error. This does not insure the quality of the  
150 extrapolation which needs additional statistics based on independent observations, i.e.  
151 observations not used by the calibration (verification data). They are provided by the  
152 observations not resampled by the bootstrap process. The prediction RMSE (called RMSEP), the  
153 reduction of error (RE) and the coefficient of efficiency (CE) are calculated on the verification  
154 data and enable to test the predictive quality of the calibrated equations (Cook et al, 1994).  
155 Traditionally, a positive RE or CE values means a statistically significant reconstruction model,

156 but bootstrap is much more interesting as it produces confidence intervals and finally we accept  
157 the RE and CE which are significantly larger than zero, which is more constraining than being  
158 just positive in mean. but bootstrap has the advantage to produce confidence intervals for such  
159 statistics without theoretical probability distribution and finally we accept the RE and CE for  
160 which the lower confidence margin at 95% are positive. This is more constraining than just  
161 accepting all positive RE and CE. An early common period (1902–1929) is available for  
162 additional verification, during which some climatic series are available but are not of sufficient  
163 quality to insure an optimal calibration. we also present traditional split-sample procedure results  
164 that divided the full period into two subsets of equal length (Meko and Graybill, 1995).

165

166 To identify the extreme March–April cold and warm events in the reconstruction, standard  
167 deviation (SD) values were used. Years one and two SD above and below the mean were  
168 identified as warm, very warm, cold, and very cold years, respectively. Finally, as a way to  
169 assess the spatial representation of our temperature reconstruction, we conducted a spatial field  
170 correlation analysis between reconstructed values and the gridded CRU TS3.23 temperature field  
171 (Jones and Harris 2008) for a broad region of the Mediterranean over the early common period  
172 (1901–1929), and over the entire instrumental period (ca. 193001–2002).

173

### 174 3 Results and Discussion

#### 175 3.1 Tree-ring chronologies

176 In addition to 15 chronologies developed by previous studies, we produced six *P. nigra*, one *P.*  
177 *sylvestris*, one *A. nordmanniana* / *P. orientalis* chronologies for this study (Table 2). The Çorum  
178 district produced two *P. nigra* chronologies: one the longest (KAR; 627 years long) and the other

179 the most sensitive to climate (SAH; mean sensitivity value of 0.25). Previous investigations of  
180 climate-tree growth relationships reported a mean sensitivity range of 0.13–0.25 for *P. nigra* in  
181 Turkey (Köse 2011, Akkemik et al. 2008). The KAR, SAH, and ERC chronologies (with mean  
182 sensitivity values from 0.22 to 0.25) were classified as very sensitive, and the SAV, HCR, and  
183 PAY chronologies (mean sensitivity values range 0.17–0.18) contained values characteristic of  
184 being sensitive to climate. The lowest mean sensitivity value was obtained for the ART A.  
185 *nordmanniana* / *P. orientalis* chronology. Nonetheless, this chronology retained a statistically  
186 significant temperature signal ( $p < 0.05$ ).

187

### 188 3.2 March-April temperature reconstruction

189 RFA coefficients of May to August precipitation are positively correlated with most of the tree-  
190 ring series (Fig. 2) and among them, May and June coefficients are generally significant. The  
191 first principal component of the 23 chronologies, which explains 47% of the tree-growth  
192 variance, is highly correlated with May–August total precipitation, statistically ( $r = 0.65, p \leq$   
193 0.001) and visually (Fig. 3). The high correlation was expected given that numerous studies also  
194 found similar results in Turkey (Akkemik 2000a, Akkemik 2000b, Akkemik 2003, Akkemik et  
195 al. 2005, [Akkemik et al. 2008](#), Akkemik & Aras 2005, Hughes et al. 2001, D'Arrigo & Cullen  
196 2001, Touchan et al. 2003; Touchan et al. 2005a, Touchan et al. 2005b, Touchan et al. 2007,  
197 Köse et al. 2011, [Köse et al. 2013](#), [Martin-Benitto et al. 2016](#)).

198

199 The influence of temperature was not as strong as May–August precipitation on radial growth,  
200 although generally positive in early spring (March and April) (Fig. 2). Conversely, the ART  
201 chronology from northeastern Turkey contained a strong temperature signal, which was

202 significantly positive in March. In addition to this chronology, we also used the chronologies that  
203 revealed the influence of precipitation, as well as temperature to reconstruct March–April  
204 temperature.

205

206 The higher order PCs of the 23 chronologies are significantly correlated with the March–April  
207 temperature and, by nature, are independent on the precipitation signal (Table 3). The best  
208 selection for fit temperature are obtained with the PC<sub>3</sub>, PC<sub>4</sub>, PC<sub>5</sub>, PC<sub>7</sub>, PC<sub>9</sub>, PC<sub>10</sub>, PC<sub>15</sub>, PC<sub>17</sub>,  
209 PC<sub>21</sub>, which explains together 25% of the tree-ring chronologies. So the temperature signal  
210 remains important in the tree-ring chronologies and can be reconstructed. The advantage to  
211 separate both signals through orthogonal PCs enable to remove an unwanted noise for our  
212 temperature reconstruction. Thus, PC<sub>1</sub> was not used as potential predictor of temperature because  
213 it is largely dominated by precipitation (Table 3, Fig. 3). The last two PCs contain a too small  
214 part of the total variance to be used in the regressions. However, even if Jolliffe (1982) and Hadi  
215 & Ling (1998) claimed that certain PCs with small eigenvalues (even the last one), which are  
216 commonly ignored by principal components regression methodology, may be related to the  
217 independent variable, we must be cautious with that because they may be much more dominated  
218 by noise than the first ones. So, the contribution of each PC to the regression sum of squares is  
219 also important for selection of PCs (Hadi & Ling 1998). The findings of Jolliffe (1982) and Hadi  
220 & Ling (1998) provide a justification for using non-primary PCs, (*e.g.*, of second and higher  
221 order) in our regression, given that correlations with temperature may be over-powered by  
222 affects from precipitation in our study area (Cook 2011, personal communication).

223

224 Using this method, the calibration and verification statistics indicated a statistically significant  
225 reconstruction (Table 4, Fig. 4). The regression model for the calibration period was: For  
226 additional verification, we also present split-sample procedure results. Similarly bootstrap  
227 results, the derived calibration and verification tests using this method indicated a statistically  
228 significant RE and CE values (Table 5).

229

230 Eq. (1):  $TMP = 7.53 - 2.94PC_3 + 4.02PC_4 + 2.50PC_5 + 2.77PC_7 + 2.73PC_9 - 2.67PC_{10} -$   
231  $5.17PC_{15} + 1.98PC_{17} - 5.82PC_{24}$

232

233 The regression model accounted for 67% (Adj.  $R^2 = 0.64$ ,  $p \leq 0.0001$ ) of the actual temperature  
234 variance over the calibration period (1930–2002). Also, actual and reconstructed March–April  
235 temperature values had nearly identical trends during the period 1930–2002 (Fig. 4). Moreover, the tree-  
236 ring chronologies successfully simulated both high frequency and warming trends in the temperature data  
237 during this period. The reconstruction was more powerful at classifying warm events rather than cold  
238 events. Over the last 73 years, eight of ten warm events in the instrumental data were also observed in  
239 the reconstruction, while five of nine cold events were captured. Similarly, previous tree-ring based  
240 precipitation reconstructions for Turkey (Köse et al. 2011; Akkemik et al. 2008) were generally  
241 more successful in capturing dry years rather than wet years.

242

243 Our temperature reconstruction on the 1800–2002 period is obtained by bootstrap regression,  
244 using 1000 iterations (Fig. 5). The confidence intervals are obtained from the range between the  
245 2.5<sup>th</sup> and the 97.5<sup>th</sup> percentiles of the 1000 simulations. For the pre-instrumental period (1800–  
246 1929), a total of 23 cold (1813, 1818, 1821, 1824, 1837, 1848, 1854, 1858, 1860, 1869, 1877–

247 1878, 1880–1881, 1883, 1897–1898, 1905–1907, 1911–1912, 1923) and 13 warm (1801–1802,  
248 1807, 1845, 1853, 1866, 1872–1873, 1879, 1885, 1890, 1901, 1926) events were determined.

249 After comparing our results with event years obtained from May–June precipitation  
250 reconstructions from western Anatolia (Köse et al. 2011), the cold years 1818, 1848, and 1897  
251 appeared to coincide with wet years and 1881 was a very wet year for the entire region.  
252 Furthermore, these years can be described as cold (in March–April) and wet (in May–June) for  
253 western Anatolia.

254

255 Spatial correlation analysis revealed that our network-based temperature reconstruction was  
256 representative of conditions across Turkey, as well as the broader Mediterranean region (Fig. 6).  
257 During the period 193001–2002, estimated temperature values were highly significant ( $r$  range  
258 0.5–0.6,  $p < 0.01$ ) with instrumental conditions recorded from southern Ukraine to the west  
259 across Romania, and from northern areas of Libya and Egypt to the east across Iraq. The strength  
260 of the reconstruction model is evident in the broad spatial implications demonstrated by the  
261 temperature record. Thus, we interpret warm and cold periods and extreme events within the  
262 record with high confidence.

263

264 Among the warm periods in our reconstruction, conditions during the year 1879 were dry, 1895  
265 wet, and 1901 very wet across the broad region of western Anatolia (Köse et al. 2011). Hence,  
266 we defined 1879 as a warm (in March–April) and dry year (in May–June), and 1895 and 1901  
267 were warm and wet years. In the years 1895 and 1901 the combination of a warm early spring  
268 and a wet late spring–summer caused enhanced radial growth in Turkey, interpreted as longer  
269 growing seasons without drought stress.

270

271 Of these event years, 1897 and 1898 were exceptionally cold and 1845, 1872 and 1873 were  
272 exceptionally warm. During the last 200 years, our reconstruction suggests that the coldest year  
273 was 1898 and the warmest year was 1873. The reconstructed extreme events also coincided with  
274 accounts from historical records. Server (2008) recounted the winter of 1898 as characterized by  
275 anomalously cold temperatures that persisted late into the spring season. A family, who brought  
276 their livestock herds up into the plateau region in Kırşehir seeking food and water were suddenly  
277 covered in snow on 11 March 1898. This account of a late spring freeze supports the  
278 reconstruction record of spring temperatures across Turkey, and offers corroboration to the  
279 quality of the reconstructed values.

280

281 Seyf (1985) reported that extreme summer temperature during the year 1873 resulted in  
282 widespread crop failure and famine. Historical documents recorded an infamous drought-derived  
283 famine that occurred in Anatolia from 1873 to 1874 (Quataert, 1996, Kuniholm, 1990), which  
284 claimed the lives of 250,000 people and a large number of cattle and sheep (Faroqhi, 2009). This  
285 drought caused widespread mortality of livestock and depopulation of rural areas through human  
286 mortality, and migration of people from rural to urban areas. Further, the German traveler  
287 Naumann (1893) reported a very dry and hot summer in Turkey during the year 1873 (Heinrich  
288 et al, 2013). Conditions worsened when the international stock exchanges crashed in 1873,  
289 marking the beginning of the "Great Depression" in the European economy (Zürcher, 2004). Our  
290 temperature record suggests that dry conditions during the early 1870s were possibly exacerbated  
291 by warm spring temperatures that likely carried into summer. A similar pattern of intensified

292 drought by warm temperatures was demonstrated recently by Griffin and Anchukaitis (2014) for  
293 the current drought in California, USA.

294

295 Extreme cold and warm events were usually one year long, and the longest extreme cold and  
296 warm events were two and three years, respectively. These results were similar with durations of  
297 extreme wet and dry events in Turkey (Touchan et al. 2003, Touchan et al. 2005a, Touchan et al.  
298 2005b, Touchan et al. 2007, Akkemik & Aras, 2005, Akkemik et al. 2005, Akkemik et al. 2008,  
299 Köse et al. 2011). Moreover, seemingly innocuous short-term warm events, such as the 1807  
300 event, were recorded across the Mediterranean and in high elevations of the European regions.  
301 Casty et al. (2005) reported the year 1807 as being one of the warmest alpine summers in the  
302 European Alps over the last 500 years. As such, a drought record from Nicault et al. (2008)  
303 echoes this finding, as a broad region of the Mediterranean basin experienced drought  
304 conditions.

305

306 Low frequency variability of our spring temperature reconstruction showed larger variability in  
307 nineteenth century than twentieth century. Similar results observed on previous tree-ring based  
308 precipitation reconstructions from Turkey (Touchan et al. 2003, D'Arrigo et al. 2001, Akkemik  
309 and Aras 2005, Akkemik et al. 2005, Köse et al. 2011). Moreover, cold periods observed in our  
310 reconstruction are generally appeared as generally wet in the precipitation reconstructions, while  
311 warm periods generally correlated with dry periods (Fig. 7).

312

313 Heinrich et al. (2013) analyzed winter-to-spring (January–May) air temperature variability in  
314 Turkey since AD 1125 as revealed from a robust tree-ring carbon isotope record from *Juniperus*

315 *excelsa*. Although they offered a long-term perspective of temperature over Turkey, the  
316 reconstruction model, which covered the period 1949–2006, explained 27% of the variance in  
317 temperature since the year 1949. In this study, we provided a short-term perspective of  
318 temperature fluctuation based on a robust model (calibrated and verified 1930–2002; Adj.  $R^2 =$   
319 0.64;  $p \leq 0.0001$ ). Yet, the Heinrich et al. (2013) temperature record did not capture the 20<sup>th</sup>  
320 century warming trend as found elsewhere (Wahl et al. 2010). However, their temperature trend  
321 does agree with trend analyses conducted on meteorological data from Turkey and other areas in  
322 the eastern Mediterranean region. The warming trend seen during our reconstruction calibration  
323 period (1930–2002) was similar to the data shown by Wahl et al. (2010) across the region and  
324 hemisphere. Further, the warming trends seen in our record agrees with data presented by Turkes  
325 & Sumer (2004), of which they attributed to increased urbanization in Turkey. Considering long-  
326 term changes in spring temperatures, the 19<sup>th</sup> century was characterized by more high-frequency  
327 fluctuations compared to the 20<sup>th</sup> century, which was defined by more gradual changes and  
328 includes the beginning of decreased DTRs in the region (Turkes & Sumer, 2004).

329

#### 330 **4 Conclusions**

331

332 In this study, we used a broad network of tree-ring chronologies to provide the first tree-ring  
333 based temperature reconstruction for Turkey and identified extreme cold and warm events during  
334 the period 1800–1929 CE. Similar to the precipitation reconstructions against which we compare  
335 our air temperature record, extreme cold and warm years were generally short in duration (one  
336 year) and rarely exceeded two-three years in duration. The coldest and warmest years over

337 western Anatolia were experienced during the 19<sup>th</sup> century, and the 20<sup>th</sup> century is marked by a  
338 temperature increase.

339

340 Reconstructed temperatures for the 19<sup>th</sup> century suggest that more short-term fluctuations  
341 occurred compared to the 20<sup>th</sup> century. The gradual warming trend shown by our reconstruction  
342 calibration period (1930–2002) is coeval with decreases in spring DTRs. Given the results of  
343 Turkes and Sumer (2004), the variations in short- and long-term temperature changes between  
344 the 19<sup>th</sup> and 20<sup>th</sup> centuries might be related to increased urbanization in Turkey.

345

346 The study revealed the potential for reconstructing temperature in an area previously thought  
347 impossible, especially given the strong precipitation signals displayed by most tree species  
348 growing in the dry Mediterranean climate that characterizes broad areas of Turkey. Our  
349 reconstruction only spans 205 years due to the shortness of the common interval for the  
350 chronologies used in this study, but the possibility exists to extend our temperature  
351 reconstruction further back in time by increasing the sample depth with more temperature-  
352 sensitive trees, especially from northeastern Turkey. Thus future research will focus on  
353 increasing the number of tree-ring sites across Turkey, and maximizing chronology length at  
354 existing sites that would ultimately extend the reconstruction back in time.

355

356

357

358

359

360 **Acknowledgements**

361

362 This research was supported by The Scientific and Technical Research Council of Turkey  
363 (TUBITAK); Projects ÇAYDAG 107Y267 and YDABAG 102Y063. N. Köse was supported by  
364 The Council of Higher Education of Turkey. We are grateful to the Turkish Forest Service  
365 personnel and Ali Kaya, Umut Ç. Kahraman and Hüseyin Yurtseven for their invaluable support  
366 during our field studies. J. Guiot was supported by the Labex OT-Med (ANR-11-LABEX-0061),  
367 French National Research Agency (ANR).

368

369 **References**

370 Akkemik, Ü.: Dendroclimatology of Umbrella pine (*Pinus pinea* L.) in Istanbul (Turkey), Tree-  
371 Ring Bull., 56, 17–20, 2000a.

372 Akkemik, Ü.: Tree-ring chronology of *Abies cilicica* Carr. in the Western Mediterranean Region  
373 of Turkey and its response to climate, Dendrochronologia, 18, 73–81, 2000b.

374 Akkemik, Ü.: Tree-rings of *Cedrus libani* A. Rich the northern boundary of its natural  
375 distribution, IAWA J, 24(1), 63-73, 2003.

376 Akkemik ,Ü and Aras, A.: Reconstruction (1689–1994) of April–August precipitation in  
377 southwestern part of central Turkey, Int. J. Clim., 25, 537–548, 2005.

378 Akkemik, Ü., Dagdeviren, N., and Aras, A.: A preliminary reconstruction (A.D. 1635–2000) of  
379 spring precipitation using oak tree rings in the western Black Sea region of Turkey, Int. J.  
380 Biomet., 49(5), 297–302, 2005.

381 Akkemik, Ü., D'Arrigo, R., Cherubini, P., Köse, N., and Jacoby, G.: Tree-ring reconstructions of  
382 precipitation and streamflow for north-western Turkey, Int. J. Clim., 28, 173–183, 2008.

383 Biondi, F. and Waikul, K.: DENDROCLIM2002: A C++ program for statistical calibration of  
384 climate signals in tree-ring chronologies, Comp. Geosci., 30, 303–311, 2004.

385 Briffa, K. R. and Jones, P. D.: Basic chronology statistics and assessment. In: Methods of  
386 Dendrochronology: Applications in the Environmental Sciences (Cook, E. and Kairiukstis, L.  
387 A. eds). Kluwer Academic Publishers, Amsterdam, pp. 137–152, 1990.

388 Casty, C., Wanner, H., Luterbacher, J., Esper, J., and Böhm, R.: Temperature and precipitation  
389 variability in the European Alps since 1500, Int. J. Clim., 25(14), 1855–1880, 2005.

390 Cook, E.: A time series analysis approach to tree-ring standardization. PhD. Dissertation.  
391 University of Arizona, Tucson, 1985.

392 Cook, E., Briffa, K., Shiyatov, S., and Mazepa, V.: Tree-ring standardization and growth-trend  
393 estimation. In: *Methods of Dendrochronology: Applications in the Environmental Sciences*  
394 (Cook, E. and Kairiukstis, L. A. eds). Kluwer Academic Publishers, Amsterdam, pp.104–  
395 122, 1990a.

396 Cook, E., Shiyatov, S., and Mazepa, V.: Estimation of the mean chronology. In: *Methods of*  
397 *Dendrochronology: Applications in the Environmental Sciences* (Cook, E. and Kairiukstis, L.  
398 A. eds). Kluwer Academic Publishers, Amsterdam, pp. 123–132, 1990b.

399 D'Arrigo, R. and Cullen, H. M.: A 350-year (AD 1628–1980) reconstruction of Turkish  
400 precipitation. *Dendrochronologia*, 19(2), 169–177, 2001.

401 Deniz, A., Toros, T., and Incecik, S.: Spatial variations of climate indices in Turkey, *Int. J.*  
402 *Clim.*, 31, 394-403, 2011.

403 Fritts, H. C.: *Tree Rings and Climate*. Academic Press, New York, 1976.

404 Griggs, C., DeGaetano, A., Kuniholm, P., and Newton, M.: A regional high-frequency  
405 reconstruction of May–June precipitation in the north Aegean from oak tree rings, A.D.  
406 1809–1989, *Int. J. Clim.*, 27, 1075–1089, 2007.

407 Grissino-Mayer, H. D.: Evaluating crossdating accuracy: A manual and tutorial for the computer  
408 program COFECHA, *Tree-Ring Res.*, 57, 205–221, 2001.

409 Griffin, D. and Anchukaitis, K. J.: How unusual is the 2012–2014 California drought? *Geophy.*  
410 *Res. Lett.*, 41(24), 9017–9023, 2014.

411 Hadi, A. S. and Ling, R. F.: Some cautionary notes on the use of principal components  
412 regression, *Amer. Statist.*, 52(1), 15–19, 1998.

413 Heinrich, I., Touchan, R., Liñán, I. D., Vos, H., and Helle, G.: Winter-to-spring temperature  
414 dynamics in Turkey derived from tree rings since AD 1125, *Clim. Dynam.*, 41(7–8), 1685–  
415 1701, 2013.

416 Holmes, R. L.: Computer-assisted quality control in tree-ring data and measurements, *Tree-Ring*  
417 *Bull.*, 43, 69–78, 1983.

418 Hughes, M. K., Kuniholm, P. I., Garfin, G. M., Latini, C., and Eischeid, J.: Aegean tree-ring  
419 signature years explained, *Tree-Ring Res.*, 57(1), 67–73, 2001.

420 Jolliffe, I. T.: A note on the use of principal components in regression, *Appl. Stat.*, 31(3), 300–  
421 303, 1982.

422 Jones, P. D. and Harris, I.: Climatic Research Unit (CRU) time-series datasets of variations in  
423 climate with variations in other phenomena. NCAS British Atmospheric Data Centre, 2008.  
424 <http://catalogue.ceda.ac.uk/uuid/3f8944800cc48e1cbc29a5ee12d8542d>

425 Köse, N., Akkemik, Ü., and Dalfes, H. N.: Anadolu'nun iklim tarihinin son 500 yılı:  
426 Dendroklimatolojik ilk sonuçlar. *Türkiye Kuvaterner Sempozyumu-TURQUA-V*, 02–03  
427 Haziran 2005, Bildiriler Kitabı, 136–142 (In Turkish), 2005.

428 Köse, N., Akkemik, Ü., Dalfes, H. N., and Özeren, M. S.: Tree-ring reconstructions of May–June  
429 precipitation of western Anatolia, *Quat. Res.*, 75, 438–450, 2011.

430 [Köse N., Akkemik U., Guner H.T., Dalfes H.N., Grissino-Mayer H.D., Ozeren M.S., Kindap T.](#)  
431 [\(2013\) An improved reconstruction of May– June precipitation using tree-ring data from](#)  
432 [western Turkey and its links to volcanic eruptions, Int. J. Biometeorol., 57\(5\):691–701](#)

433 [Martin-Benito, D., Ummenhofer C.C., Köse, N., Güner, H.T., Pederson, N. 2016. Tree-ring](#)  
434 [reconstructed May-June precipitation in the Caucasus since 1752 CE, Clim. Dyn., DOI](#)  
435 [10.1007/s00382-016-3010-1.](#)

436 Meko, D. M. and Graybill, D. A.: Tree-ring reconstruction of upper Gila River discharge, Wat.  
437 Res. Bull., 31, 605–616, 1995.

438 Mutlu, H., Köse, N., Akkemik, Ü., Aral, D., Kaya, A., Manning, S. W., Pearson, C. L., and  
439 Dalfes, N.: Environmental and climatic signals from stable isotopes in Anatolian tree rings,  
440 Turkey, Reg. Environ. Change, doi: 10.1007/s1011301102732, 2011.

441 Nicault, A., Alleaume, S., Brewer, S., Carrer, M., Nola, P., and Guiot, J.: Mediterranean drought  
442 fluctuation during the last 500 years based on tree-ring data, Clim. Dynam., 31(2–3), 227–  
443 245, 2008.

444 Orvis, K. H. and Grissino-Mayer, H. D.: Standardizing the reporting of abrasive papers used to  
445 surface tree-ring samples, Tree-Ring Res., 58, 47–50, 2002.

446 Server, M.: Evaluation of an oral history text in the context of social memory and traditional  
447 activity, Milli Folklor 77, 61–68 (In Turkish), 2008.

448 Speer, J. H.: Fundamentals of Tree-Ring Research, University of Arizona Press, Tucson, 2010.

449 Stokes, M. A. and Smiley, T. L.: An Introduction to Tree-ring Dating, The University of Arizona  
450 Press, Tucson, 1996.

451 Till, C. and Guiot, J.: Reconstruction of precipitation in Morocco since A D 1100 based on  
452 *Cedrus atlantica* tree-ring widths, Quat. Res., 33, 337–351, 1990.

453 Touchan, R., Garfin, G. M., Meko, D. M., Funkhouser, G., Erkan, N., Hughes, M. K., and  
454 Wallin, B. S.: Preliminary reconstructions of spring precipitation in southwestern Turkey  
455 from tree-ring width, Int. J. Clim., 23, 157–171, 2003.

456 Touchan, R., Xoplaki, E., Funkhouser, G., Luterbacher, J., Hughes, M. K., Erkan, N., Akkemik,  
457 Ü., and Stephan, J.: Reconstruction of spring/summer precipitation for the Eastern  
458 Mediterranean from tree-ring widths and its connection to large-scale atmospheric  
459 circulation, *Clim. Dynam.*, 25, 75–98, 2005a.

460 Touchan, R., Funkhouser, G., Hughes, M. K., and Erkan, N.: Standardized Precipitation Index  
461 reconstructed from Turkish ring widths, *Clim. Change*, 72, 339–353, 2005b.

462 Touchan, R., Akkemik, Ü., Huges, M. K., and Erkan, N.: May–June precipitation reconstruction  
463 of southwestern Anatolia, Turkey during the last 900 years from tree-rings, *Quat. Res.*, 68,  
464 196–202, 2007.

465 Turkes, M.: Spatial and temporal analysis of annual rainfall variations in Turkey. *Int. J. Clim.*,  
466 16, 1057–1076, 1996.

467 Turkes, M.: Vulnerability of Turkey to desertification with respect to precipitation and aridity  
468 conditions. *Turk. J. Engineer. Environ. Sci.*, 23, 363–380, 1999.

469 Turkes, M. and Sumer, U. M.: Spatial and temporal patterns of trends variability in diurnal  
470 temperature ranges of Turkey. *Theor. Appl. Clim.*, 77, 195–227, 2004.

471 Wahl, E. R., Anderson, D. M., Bauer, B. A., Buckner, R., Gille, E. P., Gross, W. S., Hartman,  
472 M., and Shah, A.: An archive of high-resolution temperature reconstructions over the past  
473 two millennia, *Geochem. Geophys. Geosyst.*, 11, Q01001, doi:10.1029/2009GC002817,  
474 2010.

475 Wigley, T. M. L., Briffa, K. R., and Jones, P. D.: On the average value of correlated time series  
476 with applications in dendroclimatology and hydrometeorology, *J. Clim. Appl. Met.*, 23, 201–  
477 213, 1984.

478 Yamaguchi, D. K.: A simple method for cross-dating increment cores from living trees. *Can. J.*  
479 *For. Res.*, 21, 414–416, 1991.

480 Table 1. Site information for the new chronologies developed by this study in Turkey.

Site name	Site code	Species	No. trees/cores	Aspect	Elev. (m)	Lat. (N)	Long. (E)
Çorum, Kargı, Karakise kayalıkları	KAR	<i>Pinus nigra</i>	22 / 38	SW	1522	41°11'	34°28'
Çorum, Kargı, Şahinkayası mevkii	SAH	<i>P. nigra</i>	12 / 21	S	1300	41°13'	34°47'
Bilecik, Muratdere	ERC	<i>P. nigra</i>	12 / 25	SE	1240	39°53'	29°50'
Bolu, Yedigöller, Ayıkaya mevkii	BOL	<i>P. sylvestris</i>	10 / 20	SW	1702	40°53'	31°40'
Eskişehir, Mihalıççık, Savaş alanı mevkii	SAV	<i>P. nigra</i>	10 / 18	S	1558	39°57'	31°12'
Kayseri, Aladağlar milli parkı, Hacer ormanı	HCR	<i>P. nigra</i>	18 / 33	S	1884	37°49'	35°17'
Kahramanmaraş, Göksun, Payanburnu mevkii	PAY	<i>P. nigra</i>	10 / 17	S	1367	37°52'	36°21'
Artvin, Borçka, Balcı işletmesi	ART	<i>Abies nordmanniana</i> <i>Picea orientalis</i>	23 / 45	N	1200–2100	41°18'	41°54'

481

482

483

Table 2. Summary statistics for the new chronologies developed by this study in Turkey.

Site Code	Time span	Total chronology		Common interval		
		1st year (*EPS > 0.85)	Mean sensitivity	Time span	Mean correlations: among radii /between radii and mean	Variance explained by PC1 (%)
KAR	1307– 2003	1620	0.22	1740–1994	0.38 / 0.63	41
SAH	1663– 2003	1738	0.25	1799–2000	0.42 / 0.67	45
ERC	1721– 2008	1721	0.23	1837–2008	0.45 / 0.69	48
BOL	1752– 2009	1801	0.18	1839–1994	0.32 / 0.60	36
SAV	1630– 2005	1700	0.17	1775–2000	0.33 / 0.60	38
HCR	1532– 2010	1704	0.18	1730–2010	0.38 / 0.63	40
PAY	1537– 2010	1790	0.18	1880–2010	0.28 / 0.56	32
ART	1498– 2007	1624	0.12	1739–1996	0.37 / 0.60	41

484

\*EPS = Expressed Population Signal [Wigley et al., 1984]

485

486 Table 3. Statistics from reconstruction model principal components analysis.

	Explained variance (%)	Correlation coefficients with		The chronologies represented by higher magnitudes** in the eigenvectors
		May–August PPT	March–April TMP	
PC1	46.57	0.65	0.19	KAR, KIZ, TEF, BON, USA, TUR, CAT, INC, ERC, YAU, SAV, TAN, SIU
PC2	7.86	-0.07	0.15	KAR, SAV, TIR, BOL, YAU, ESK, TEF, BON, SIU
PC3*	4.93	0.04	-0.48	HCR, PAY, BOL, YAU, SIA
PC4*	4.68	0.11	0.17	TEF, KEL, FIR, SIA, KIZ, SIU, ART
PC5*	4.42	-0.25	0.27	SAH, TIR, FIR, ART
PC6	3.73	0.15	-0.14	KIZ, FIR, SAV, KAR, TIR, PAY, ESK, TEF, BON, ART
PC7*	3.56	0.19	0.18	KIZ, BON, BOL, YAU, HCR, PAY, INC
PC8	2.87	0.26	0.01	HCR, ESK, BON, FIR, ERC, SIA
PC9*	2.45	0.16	0.17	PAY, USA, BOL, YAU, TIR, HCR, FIR, SIA, SIU
PC10*	2.21	0.14	-0.08	TUR, CAT, SAV, SIA, KEL, ERC, SIU
PC11	2.09	-0.36	-0.20	HCR, TEF, USA, INC, PAY, TUR, SAV, SIU
PC12	1.80	-0.12	0.05	TEF, CAT, YAU, HCR, ESK, USA, BOL, SIA
PC13	1.63	-0.06	0.17	TEF, TUR, BOL, KAR, YAU, SIA
PC14	1.55	-0.14	0.06	TIR, USA, FIR, TUR, YAU, KAR, BON
PC15*	1.50	-0.20	-0.14	KIZ, BON, USA, ESK, INC, BOL
PC16	1.31	0.04	0.08	SAH, HCR, INC, YAU, SAV, KAR, FIR, BOL, SIU
PC17*	1.25	0.15	0.19	SAH, SIU, KAR, ESK, TUR, ERC
PC18	1.14	0.13	0.02	KAR, TEF, TUR, SAV, BON, CAT
PC19	1.09	0.16	-0.11	PAY, INC, SAV, HCR, KEL, CAT, TAN
PC20	0.95	-0.15	-0.01	TIR, SAH, CAT
PC21*	0.89	0.06	-0.28	TUR, INC, TIR, SAV
PC22	0.85	0.44	0.10	KIZ, SAH, BON, YAU, SIU
PC23	0.67	-0.22	-0.02	TAN, KEL, TUR, CAT

487 “\*\*” indicates the PCs, which used in the reconstruction as predictors

488 “\*\*” which exceed  $\pm 0.2$  value.

489

490

491

492

493

494 Table 4. Calibration and verification statistics of bootstrap method (1000 iterations  
495 applied) showing the mean values based on the 95% confidence interval (CI)

496

Mean (95% CI)		
Calibration	RMSE	0.65 (0.52; 0.77)
	$R^2$	0.73 (0.60; 0.83)
Verification	RE	0.54 (0.15; 0.74)
	CE	0.51 (0.04; 0.72)
	RMSEP	0.88 (0.67; 1.09)

497 *RMSE* root mean squared error;  $R^2$  coefficient of determination; *RE* reduction of error; *CE*  
498 coefficient of efficiency; *RMSEP* root mean squared error prediction

499

500

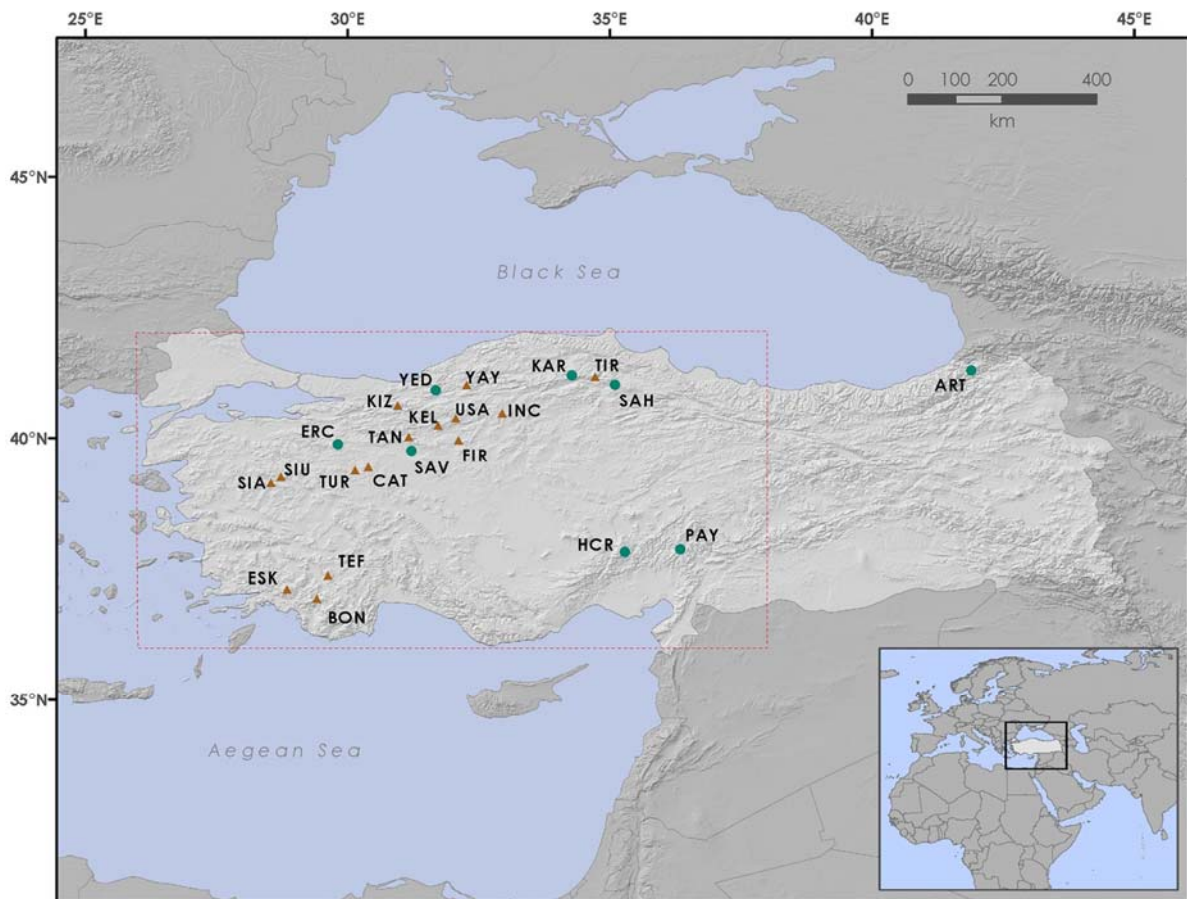
501 [Table 5. Results of the statistical calibrations and cross-validations between March–April](#)  
502 [temperature and tree growth](#)

Calibration Period	Verification Period	Adj. $R^2$	F	RE	CE
1930–1966	1967–2002	0.55	5.91	0.64	0.58
			$p \leq 0.0001$		
1967–2002	1930–1966	0.71	10.45	0.63	0.46
			$p \leq 0.0001$		

503

504

505

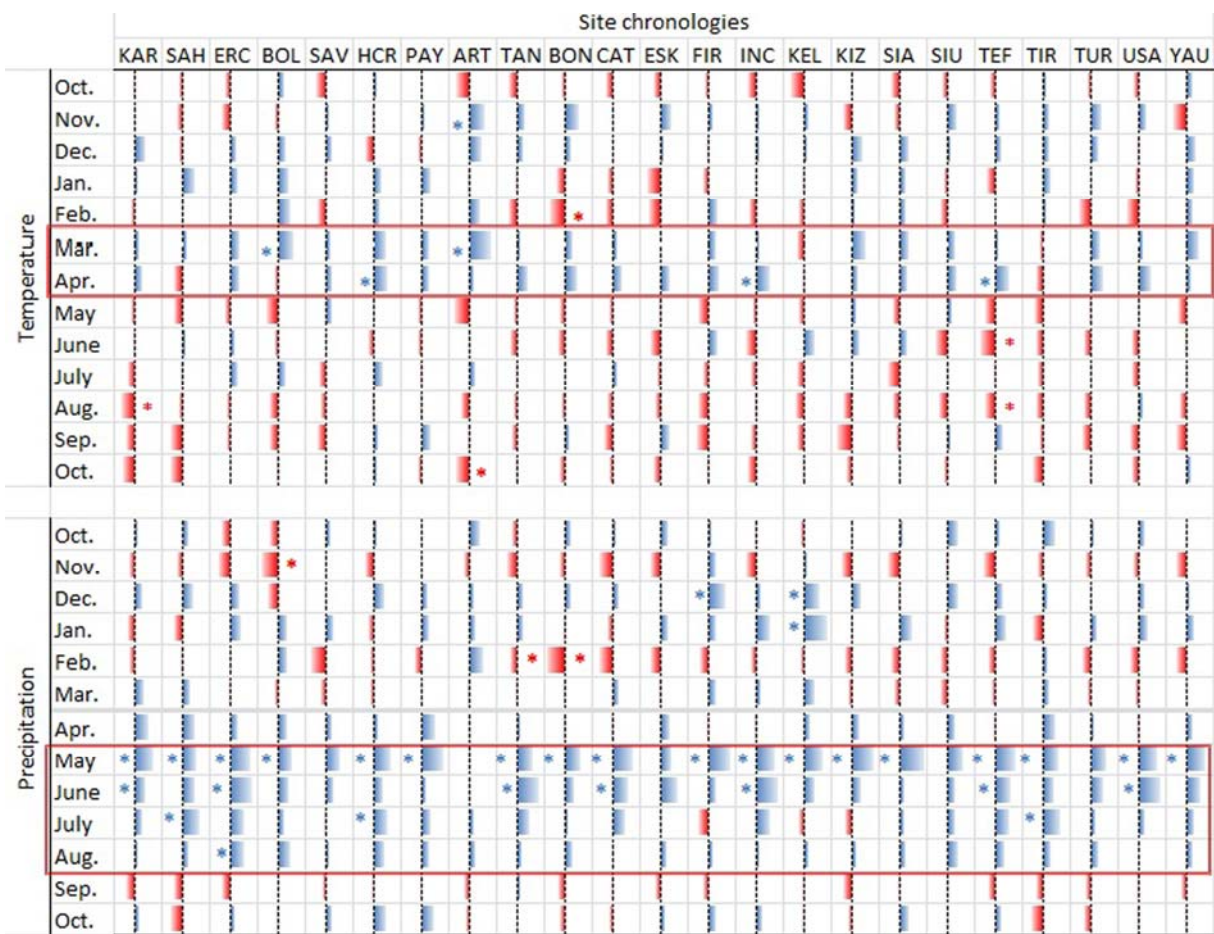


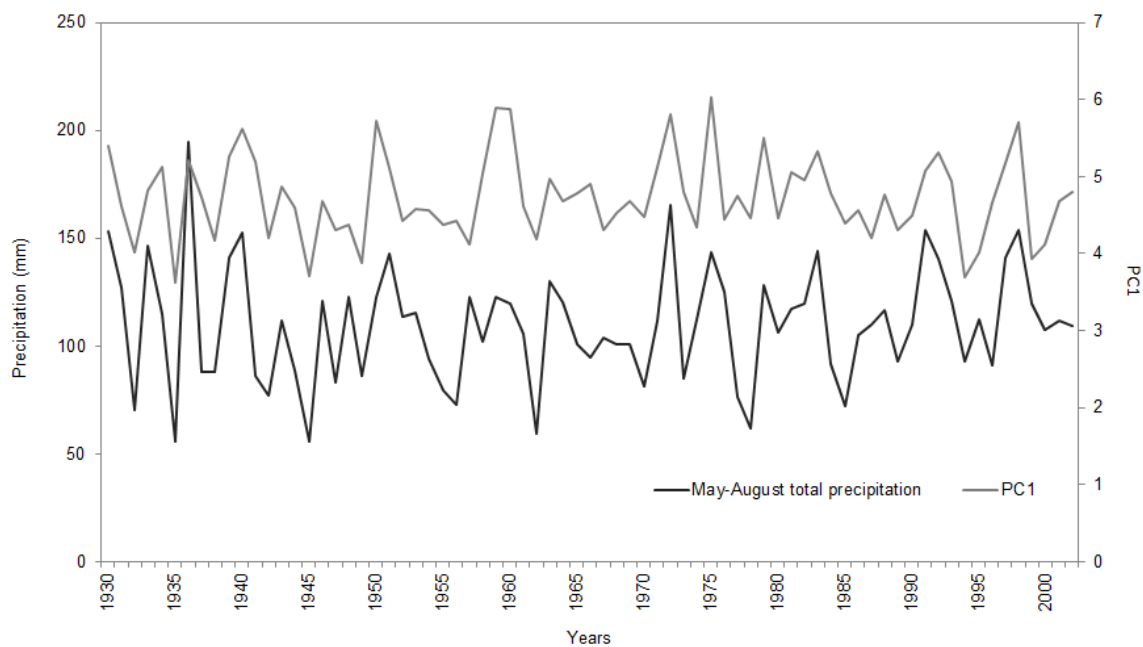
506  
507 **Figure 1.** Tree-ring chronology sites in Turkey used to reconstruct temperature. Circles  
508 represent the new sampling efforts from this study and the triangles represent previously-  
509 published chronologies (YAY, SIA, SIU: Mutlu et al. 2011; TIR: Akkemik et al. 2008; TAN:  
510 Köse et al. unpublished data; KIZ, ESK, TEF, BON, KEL, USA, FIR, TUR: Köse et al. 2011;  
511 CAT, INC: Köse et al. 2005). The box (dashed line) represents the area for which the  
512 temperature reconstruction was performed.

513

514

515





523

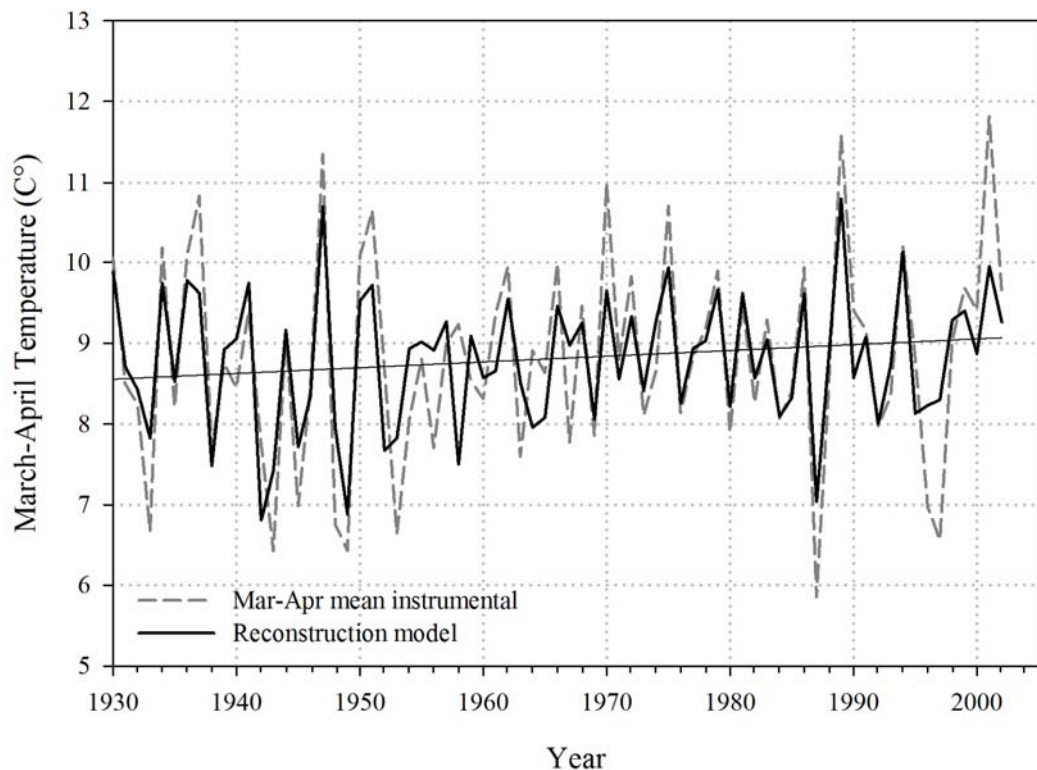
524 **Figure 3.** The comparison of May-August total precipitation (mm) and the first principal  
 525 component of 23 tree-ring chronologies.

526

527

528

529



530

531 **Figure 4.** Actual (instrumental) and reconstructed March–April temperature (°C). Dashed lines  
 532 (dark grey) represent actual values and solid lines (black) represent reconstructed values shown  
 533 with trend line (linear black line). Note: y-axes labels range 5–13 °C.

534

535

536

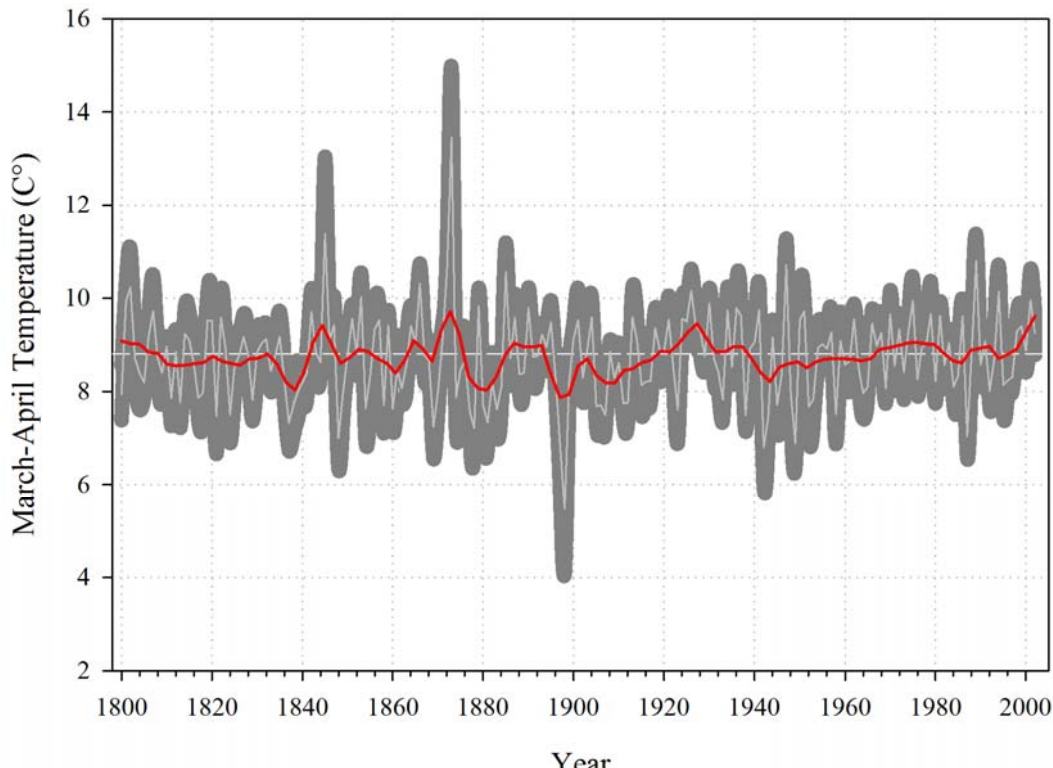
537

538

539

540

541



542

543 **Figure 5.** March–April temperature reconstruction for Turkey for the period 1800–2002

544 CE. The central horizontal line (dashed white) shows the reconstructed long-term mean;

545 dark grey background denotes Monte Carlo ( $n = 1000$ ) bootstrapped 95% confidence

546 limits; and the solid black line shows 13-year low-pass filter values. Note: y-axis labels

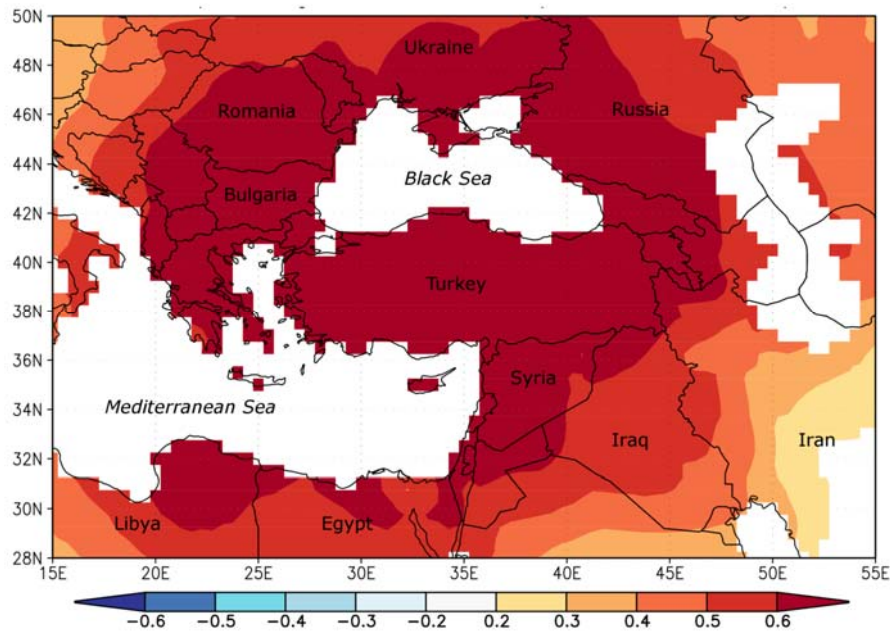
547 range 2–16 °C.

548

549

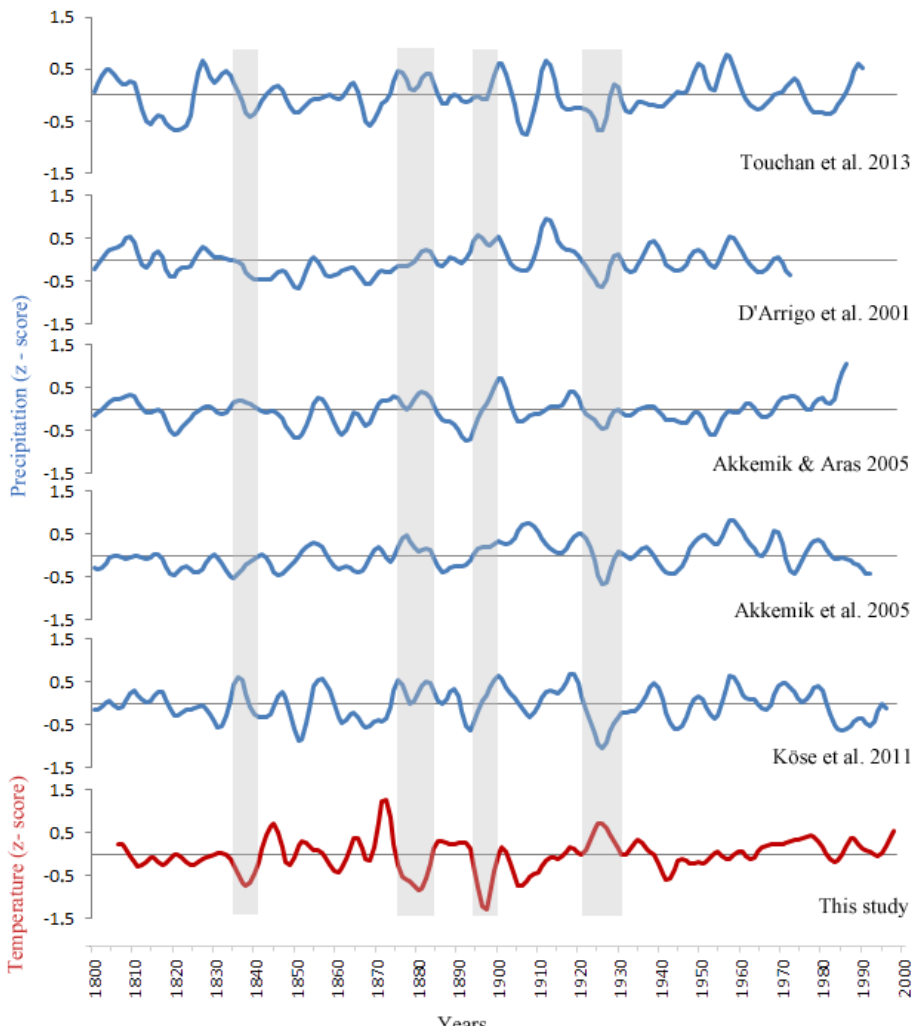
550

551



552

553 **Figure 6.** Spatial correlation map for the March–April temperature reconstruction. Spatial  
 554 field correlation map showing statistical relationship between the temperature  
 555 reconstruction and the gridded temperature field at  $0.5^{\circ}$  intervals (CRU TS3.23; Jones and  
 556 Harris 2008) during the period 1930–2002 [\[A\]](#) and ~~1901–1929~~ [\[B\]](#) over the Mediterranean  
 557 region.



558

559 **Figure 7.** Low-frequency variability of previous tree-ring based precipitation

560 reconstructions from Turkey and spring temperature reconstruction. Each line shows 13-

561 year low-pass filter values. z-scores were used for comparison.

562